

# APPLICATIONS OF NEURAL NETWORK AND NEURO-FUZZY NETWORK TO ESTIMATE THE PARAMETERS OF SELF-COMPACTING CONCRETE

Cuong Hung Nguyen<sup>1</sup>, and\**Linh Hoai Tran*<sup>2</sup>

<sup>1</sup>Hanoi University of Civil Engineering, Faculty of Building and Industrial Construction, Vietnam;

<sup>2</sup>Hanoi University of Science and Technology, School of Electrical and Electronics Engineering, Vietnam

\*Corresponding Author, Received: 21 Oct. 2022, Revised: 01 March 2023, Accepted: 24 March 2023

**ABSTRACT:** The paper presents the new application of two classical nonlinear estimators, which are the multi layer perceptron and the neuro-fuzzy networks, to approximate the workability parameters of fresh self-compacting concrete based on the amount of input ingredients like cement, fly ash, water, additives or admixtures. The estimation of workability parameters is much needed to determine the quality of the fresh self-compacting concrete before starting the production. A total of 360 real field tests of 30 types of self-compacting concrete were conducted and seven basic parameters were measured for each test. These samples will form the training and testing data sets for the nonlinear models. The numerical results showed that the MLP network could estimate the workability parameters with relative errors less than 3.6% and the TSK could estimate with relative errors less than 2.7%. These results proved the ability to create high accuracy approximation models of the proposed solutions, where the neuro-fuzzy model would show a little better performance than the multilayer perceptron. Both of the models required only relatively simple structures, making them more promising to be used in practical applications.

*Keywords: Self-compacting concrete; Nonlinear approximation; Neuro-fuzzy network; Multilayer perceptron*

## 1. INTRODUCTION

Self-compacting concrete (SCC) is a fresh concrete mixture with high flexibility, self-flowing under the weight to completely fill all edges of the form without vibration, passing through complex geometry without being segregated. The performance of self-compacting concrete is affected by climatic conditions (temperature and humidity), its workability will decrease over time, especially under high temperature and low humidity conditions, so the advantages of self-compacting concrete will no longer be the same. The decrease of workability not only affects the difficulty of construction but also affects the quality and strength of self-compacting concrete [1, 2].

Vietnam has a tropical monsoon climate, and many unfavorable weather cycles have negative impacts on the workability of self-compacting concrete such as hot weather, dry. Therefore, there is an urgent need to study and develop a model to predict the variation of SCC parameters in Vietnamese climate. In practice, computational models for estimating the workability parameters of the SCC based on the input components are highly expected. Currently, SCCs are created using predefined fixed mixes of input components, so any change to SCC parameters requires retesting a number of scenarios of mixed input components, which is time consuming and expensive. High-precision calculation models help to quickly

estimate the outcomes of the workability parameters, thereby significantly reducing the time to find new mix ratios and the cost of actual field trials and tests.

In this paper, we introduce and compare two methods using artificial neural network (ANN) and neuro-fuzzy network to predict SCC parameters [3, 4] depending on the amount of main components such as cement, fly ash, water, super ductile additive (SD) and viscosity modifying admixtures (VMA). The SCC parameters considered in this paper are the 7 most popular ones namely slump flow ( $SF$ ),  $t_{500}$ ,  $V_{funel}$ ,  $L_{box}$ ,  $J_{ring}$ , segregation ratio ( $SR$ ) and  $R_{28}$  [5, 6, 7].

There have been various studies and resulting models to estimate the parameters of SCC, among which the compressive strength  $R_{28}$  is the most commonly considered parameter. Various models based on different input sets have been proposed just to predict the  $R_{28}$ . For example,  $R_{28}$  was predicted in [8] based on 4 inputs: the water/binder (W/B) ratio, the control compressive strength, the percentage of plastic replacement and the plastic type. But in [9],  $R_{28}$  is predicted from on the W/B ratio and 6 other inputs, and in [10] the number of inputs is increased to 15. The work of [7] used 7 inputs such as cement, blast furnace slag, fly ash, water, superplasticizer, coarse aggregate, and fine aggregate to predict  $R_{28}$ . A distinct approach is proposed in [11], where  $R_{28}$  is predicted from some of the workability parameters themselves, such as

$SF$ ,  $V_{funnel}$ ,  $L_{box}$ . The proposed model in this paper achieves a correlation coefficient of 0.976.

When the  $R_{28}$  is the most popular parameter that is under consideration for many studies, we found that not much models were investigated for the other six parameters. Additionally, the studies have highlighted that the workability parameters' dependencies on the inputs undergo changes when the production technique is altered or new admixtures are introduced, leading to the need for models update or re-training with new data.

For the purpose of this article, we experimentally mixed 360 SCC samples to create a data sample set using the required standard procedures and measuring gages. As nonlinear estimators, the neural network and the neuro-fuzzy network were used and tested. Two networks were trained to generate all 7 workability parameters of SCC from the input amounts of the selected components listed above. These models are classic and have achieved good success on various technical problems [3, 4, 7, 12, 13, 14]. Both models are adaptive, meaning their parameters can be adapted to fit a given data samples. Numerical results showed that both neural networks and neuro-fuzzy networks can be used as good nonlinear estimators for the workability parameters of SCC, with neuro-fuzzy network performing slightly better.

## 2. THE WORKABILITY PARAMETERS OF SELF-COMPACTING CONCRETE

The SCC parameters selected in this paper to be estimated by the computational models, are defined in EN 12350 [5], and the 7 most popular parameters were listed in the Introduction section. They are described in more detail below.

The SF (*Slump flow*) and  $t_{500}$  time are determined in the tests described in EN 12350-2 to assess the fillability of SCC in the absence of obstruction. A simplified scheme is presented in Fig. 1, where the SCC is released from the collar and allowed to spread out and expand. The  $t_{500}$  is the time (rounded to 0.1s) required for the SCC to first reach a 500-mm diameter circle, for example at point A in Fig. 1. The  $t_{500}$  time indicates also the relative viscosity of the SCC. Thereafter, the SCC continued to spread, and when it stopped, the diameters of the SCC are measured.

The SF parameter is defined as:

$$SF = \frac{d_1 + d_2}{2} \quad (1)$$

where  $d_1$  is the SCC area diameter and  $d_2$  is the dimension perpendicular to  $d_1$  as shown in Fig. 1.

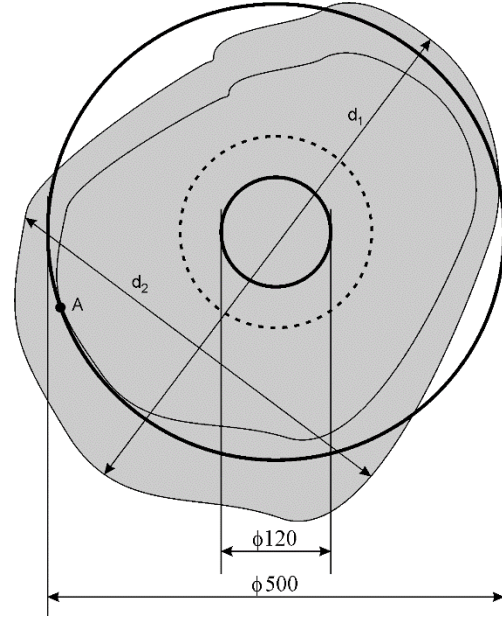


Fig.1 The description of the parameters used in the SF test

The  $V_{funnel}$  parameter is the time needed by the SCC to flow out completely from a fully filled V-shaped funnel. An example of V-shaped funnel is shown in Fig. 2. The  $V_{funnel}$  time is also rounded to 0.1s.

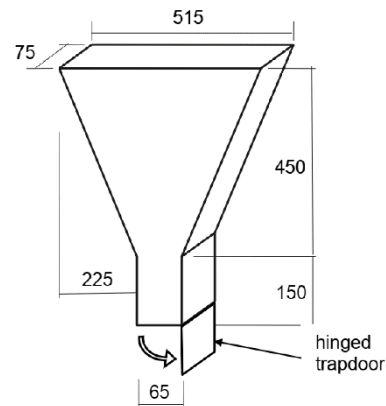


Fig. 2. The design of the V-shaped funnel and an example of its use in practical [5]

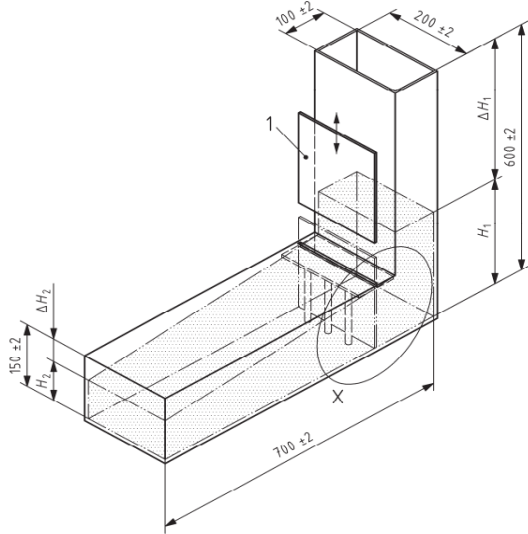


Fig. 3. The design of the L-shaped box and an example of its use in practice

The  $L_{box}$  parameter is the ratio of the heights of the concrete at both ends after letting the concrete to spread inside an L-shape box. This parameter indicates the ability of the SCC to pass through narrow openings such as spaces between the reinforcement bars in the building structure.

The resistance of the SCC to segregation is tested in the sieve segregation test. In this test, fresh SCC is allowed to stand for approximately 15 minutes, then the top portion of the sample is taken and poured into a 5mm sieve. The ratio between the material passing through the grid and the poured mass is called the segregation ratio:

$$SR = \frac{(m_{ps} - m_p) \cdot 100}{m_c} \quad (2)$$

where:  $m_{ps}$  is the mass of the SFC passed (including the sieve receiver, measured in grams),  $m_p$  is the mass of the sieve receiver itself, and  $m_c$  is the input mass of SFC.

The  $J_{ring}$  test is used to test the SCC's ability to pass when obstruction occurs. Fresh SCC is pured in to a slump cone standing on a stiff, square base plate. A  $J_{ring}$  device as shown on Fig. 4 is used to

simulate the obstructions. The  $J_{ring}$  device is placed in the center with the slump cone inside. Once the SCC is placed inside the cone, the cone is raised vertically to allow the concrete to flow out through the ring.

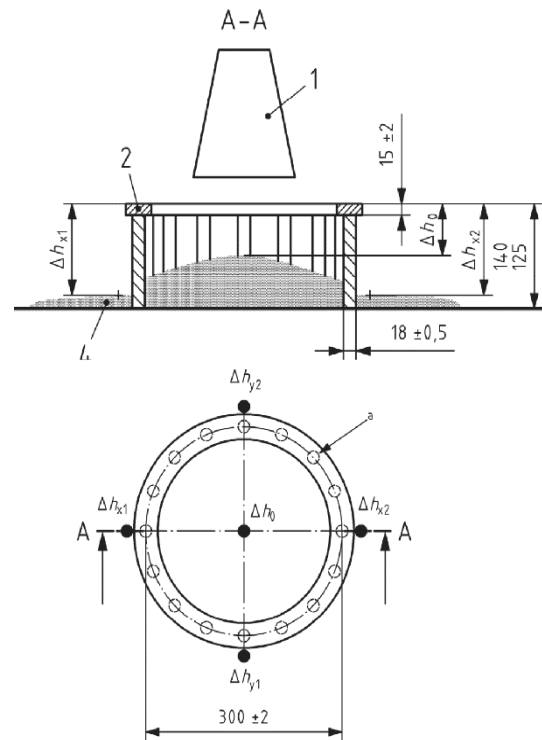


Fig. 4. The use of a  $J_{ring}$  in practical test and its design with marked characteristic points and values

The 5 distances from the level of the top of the ring to the top of the spreaded SCC were measured:

- The gap distance at the center of the  $J_{ring}$  device  $\Delta h_0$
- The two distances at just outside of the west and east farthest points of the  $J_{ring}$  device (along horizontal axis)  $\Delta h_{x1}$  and  $\Delta h_{x2}$ .
- The two distances right outside of the north and south farthest points of the  $J_{ring}$  device (along vertical axis)  $\Delta h_{y1}$  and  $\Delta h_{y2}$ .

Table 1 Examples of measured parameters of SCC

Type	Cement (kg)	Fly ash (kg)	Water (kg)	SD (kg)	VMA (kg)	SF (mm)	t <sub>500</sub> (s)	V <sub>funel</sub> (s)	SR	L <sub>box</sub>	J <sub>ring</sub> (mm)	R <sub>28</sub> (Mpa)
CP1	600.0	52.9	197.0	6.53	0.23	600	5	12.4	4.6	0.8	<u>10.7</u>	67.9
CP2	576.8	50.8	189.0	6.28	0.22	605	4.2	11.6	7.8	0.8	<u>10.5</u>	64.7
CP3	546.0	48.1	187.1	5.94	0.21	630	3.1	10.2	8.9	0.81	10	63.8
CP4	518.3	45.7	197.4	5.64	0.20	672	2.87	9.7	11.7	0.82	10	52.6
CP5	500.9	44.1	203.8	5.45	0.19	685	2.34	9.34	12.8	0.83	9.9	49.8
CP6	548.7	96.8	199.0	6.45	0.22	635	4.95	11.7	5.9	0.81	10	60.6
CP7	527.7	93.1	192.0	6.21	0.21	640	4.9	11.8	6.5	0.82	10	60.3
CP8	499.8	88.2	185.2	5.88	0.20	660	4.8	11.2	7.3	0.87	9.9	56.9
CP9	474.7	83.8	195.5	5.58	0.19	680	3.9	9.7	8.6	0.82	9.8	55.4
CP10	458.9	81.0	201.9	5.40	0.19	710	1.74	8.1	17	0.92	9.5	48.5
CP11	476.3	158.8	201.0	6.35	0.22	655	4.7	9.45	7.2	0.94	9.3	59.5
CP12	458.3	152.8	194.0	6.11	0.21	660	4.67	9.34	7.2	0.95	9.1	57.2
CP13	434.4	144.8	182.5	5.79	0.20	690	4.8	9.87	6.9	0.82	9.4	52.1
CP14	412.9	137.6	192.7	5.51	0.19	705	4.65	9.3	9.1	0.84	9.1	50.1
CP15	399.4	133.1	199.2	5.33	0.18	720	1.6	7.5	19.5	0.94	9	47.8
CP16	406.2	218.7	205.0	6.25	0.22	690	3.15	9.15	8.5	0.88	9.5	46.9
CP17	391.1	210.6	196.0	6.02	0.21	695	3.1	9.2	8.6	0.87	9.6	46
CP18	371.0	199.8	179.8	5.71	0.20	700	2.78	8.9	8.7	0.89	9.5	46.3
CP19	352.9	190.0	190.0	5.43	0.19	730	1.67	7.3	15.7	0.92	9.1	44.9
CP20	341.5	183.9	196.5	5.25	0.18	740	1.42	6.8	18	0.957	8.9	41.5
CP21	359.8	258.4	205.0	6.18	0.21	750	3	8.9	7	0.91	9.2	44.1
CP22	346.6	248.9	198.0	5.95	0.21	768	3.1	9	7.2	0.91	9.3	44.5
CP23	329.0	236.3	188.0	5.65	0.20	770	3.2	9.1	7.3	0.92	9.4	44.9
CP24	313.0	224.8	188.3	5.38	0.19	805	1.5	7	19	0.92	7.9	43.7
CP25	303.0	217.6	194.7	5.21	0.18	810	1.52	6.7	19.7	0.98	7.8	42.3
CP26	409.3	140.0	197.0	5.49	0.19	710	4.56	9.2	8.7	0.85	9	49.4
CP27	399.9	133.0	211.0	5.33	0.18	715	1.56	7.6	20	0.947	9.5	47.7
CP28	444.9	147.4	185.9	5.92	0.20	650	4.79	9.7	7.56	0.957	9.2	58.1
CP29	328.8	236.4	189.0	5.65	0.20	795	2.44	8.79	5.1	1	9.2	45.1
CP30	323.9	216.0	192.0	5.40	0.19	800	1.54	7.7	20	0.9	8	44.8

With these 5 distances, the  $J_{ring}$  value is calculated as:

$$J_{ring} = \frac{\Delta h_{x1} + \Delta h_{x2} + \Delta h_{y1} + \Delta h_{y2}}{4} - \Delta h_0 \quad (3)$$

This value should be less than 10mm for the SCC to be accepted.

The last parameter, the  $R_{28}$ , is used to evaluate the effect of the storage time of the concrete mixture on the compression resistance rate of the concrete. Samples of concrete mixture were collected every 30 minutes. These samples were kept under standard conditions and tested on a spindle compressor after 28 days.

The working parameters of self-compacting concrete mixture depend on the amounts of input components, where we tested with the variations of 5 main components: cement, fly ash, water, SD and VMA. All the tests had 770kg of rocks and 808kg of sands. We tested 30 main types of SCC, whose examples ingredients are given in Tab. 1. For each type, we repeated the tests with small variations in the input ingredients to created a total of 360 data samples.

As it can be deduced from the measurement results, the parameters of SCC strongly depend nonlinearly on the input components [3, 6]. The need of a mathematical model predicting the parameters from the input ingredients is very high because thanks to the generalization ability of the model, we can predict the parameters for the input conditions, which were not presented in the learning data samples [15]. In this paper, we proposed to use the classic MultiLayer Perceptron (MLP) and the neuro-fuzzy Takaga – Sugeno – Kang (TSK) network as the non-linear estimators.

### 3. THE NEURAL NETWORK AND NEURO-FUZZY NETWORK AS NONLINEAR ESTIMATORS

In a typical approach of using machine learning algorithms to create new models for approximation, estimation or classification of objects of unknown transfer functions mapping from inputs to the output, the models are adapted in the supervised mode, based on two data sets, the learning and testing set. If we denoted the learning data samples set containing  $p$  pairs of input-output  $\{\mathbf{x}_i, \mathbf{d}_i\}$  where  $i = 1, \dots, p$ ;  $\mathbf{x}_i \in \square^N$ ;  $\mathbf{d}_i \in \square^K$  then the parameters of an estimating function  $f()$  are adapted to minimize the error function:

$$E_{learn} = \frac{1}{2} \sum_{i=1}^p \|f(\mathbf{x}_i) - \mathbf{d}_i\|^2 \rightarrow \min \quad (4)$$

After that, the function is tested with new set of  $q$  pairs of data  $\{\mathbf{x}_i^{test}, \mathbf{d}_i^{test}\}$  where  $i = 1, \dots, q$ :

$$E_{test} = \frac{1}{2} \sum_{i=1}^q \|f(\mathbf{x}_i^{test}) - \mathbf{d}_i^{test}\|^2 \quad (5)$$

If there are different candidates for the estimator, the one with lowest testing error will be selected as the winner.

The MLP (*MultiLayer Perceptron*) is a feedforward structure with cascaded layers [15, 16]. The network with 1 input layer, 1 output layer and 1 hidden layer is the most popular in applications. In Fig. 5 an example of MLP network with only 1 hidden layer is presented with  $N$  inputs (and one constant input "1"),  $M$  neurons in the hidden layer and  $K$  outputs; the connections between the inputs and the hidden neurons are denoted by  $W_{ij}$  ( $i = 1, 2, \dots, M$ ;  $j = 0, 1, 2, \dots, N$ ), the connections between the hidden neurons and the outputs are denoted by  $V_{ij}$  ( $i = 1, 2, \dots, K$ ;  $j = 0, 1, 2, \dots, M$ ). the transfer function of hidden neurons is  $f_1$  and the transfer function of output neurons is  $f_2$ .

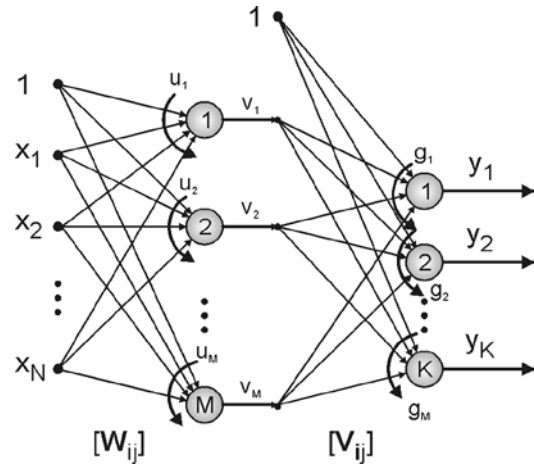


Fig. 5. An example of MLP with one hidden layer

The output of the MLP is calculated as a feedforward network for an input vector  $\mathbf{x} = [x_1, x_2, \dots, x_N] \in \square^N$  as follow:

- Outputs of hidden layer's neurons  $v_i$  for  $i = 1, \dots, M$  :

$$\begin{cases} v_0 = 0 \\ v_i = f_1 \left( \sum_{j=0}^M x_j W_{ij} \right) \end{cases} \quad (6)$$

- Outputs of the MLP network  $y_i$  for  $i = 1, \dots, K$  :

$$y_i = f_2 \left( \sum_{j=0}^M v_j V_{ij} \right) \quad (7)$$

or in a simplified form as:

$$y_i = f_2 \left( \sum_{j=0}^N \left[ f_1 \left( \sum_{k=0}^N x_k W_{jk} \right) V_{ij} \right] \right) \quad (8)$$

This network is widely used for nonlinear mapping problems [3, 4, 13]. When a structure with a given number of hidden neurons is trained to fit a set of learning data samples, the weights  $W_{ij}$  and  $V_{ij}$  are adjusted. The classic Levenberg – Marquadt algorithm was used to train the MLPs [15, 16]. The number of hidden neurons was chosen by the trial and error method, i.e. a number of networks were randomly generated, then trained on the same set of samples and tested with another set of samples. The network with lowest test error would be selected for further application. We started testing from a network with only 1 hidden neuron and successively increased the number of hidden neurons since simple networks correspond to lower VC dimensions and better performance in testing [15].

The second nonlinear estimator that is used for testing in this paper is the well-known model of neuro-fuzzy TSK network, whose structure is given in Fig. 6 with  $N$  inputs,  $M$  reasoning rules and 1 output (for simplification since the model can be defined for any outputs number).

The output of the TSK for an input vector  $\mathbf{x} = [x_1, x_2, \dots, x_N] \in \mathbb{R}^N$  is determined as follow:

- The output of each elementary fuzzifier  $\mu_i(x_j)$  realizing the fuzzy value of  $x_j \approx A_{ij}$  for  $i = 1, \dots, M$ ,  $j = 1, \dots, N$ :

$$\mu_i(x_j) = \frac{1}{1 + \left( \frac{x_j - A_{ij}}{\sigma_{ij}} \right)^{2b_{ij}}} \quad (9)$$

- The output of the fuzzifiers denoted as  $\mu_i(\mathbf{x})$  for  $i = 1, \dots, M$ :

$$\mu_i(\mathbf{x}) = \prod_{j=1}^N \mu_i(x_j) = \prod_{j=1}^N \frac{1}{1 + \left( \frac{x_j - A_{ij}}{\sigma_{ij}} \right)^{2b_{ij}}} \quad (10)$$

where  $A_{ij}$ ,  $\sigma_{ij}$  and  $b_{ij}$  are nonlinear parameters to be trained.

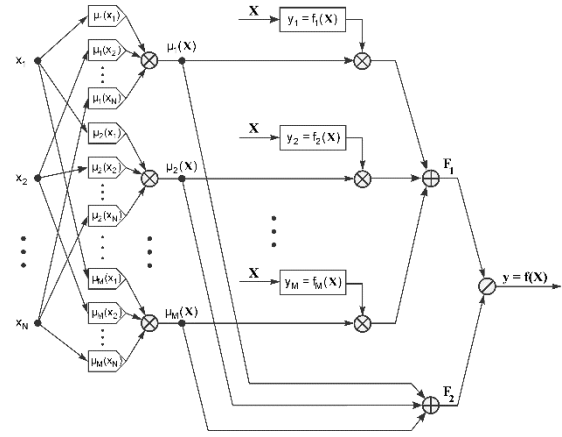


Fig. 6. An example of TSK network with one output

- The output of linear TSK function denoted as  $f_i(\mathbf{x})$  for  $i = 1, \dots, M$ :

$$f_i(\mathbf{x}) = q_{i0} + \sum_{j=1}^N q_{ij} x_j \quad (11)$$

where  $q_{ij}$  are linear parameters to be trained.

- The output of the TSK network:

$$y = \frac{F_1}{F_2} = \frac{\sum_{i=1}^M \mu_i(\mathbf{x}) \cdot f_i(\mathbf{x})}{\sum_{i=1}^M \mu_i(\mathbf{x})} \quad (12)$$

For the TSK network, similar to the MLP network, the number of inputs and outputs are defined by the data samples. During the training it's needed to find the number of rules that could allow the network to achieve satisfactory low level of testing errors. We used the similar "trial and test" approach, starting with network with only 1 rule and increase the number of rules during the trials. To train the TSK networks, the hybrid algorithm described in [16] was used.

#### 4. NUMERICAL EXPERIMENTS AND RESULTS

Experimentally 360 SCC samples (12 variants of each of 30 types of SCC as listed in Tab. 1) were mixed and tested. For each type of SCC, 10 variants were randomly selected to the training set, the remaining 2 were assigned to the testing set. The goal of the training is to build a model that replicates the nonlinear mapping between the inputs (the amount of each components) and the outputs (the workability parameters of the mixed SCC).

Totally, the training set had 300 samples, the testing set had 60 samples. As measures of accuracy, we used following indicators calculated for the testing data set (as mentioned in previous section, the error on the testing data set is more important):

- MAE (*Mean Absolute Error*):

$$MAE = \frac{1}{q} \sum_{i=1}^q \| \mathbf{y}_i^{test} - \mathbf{d}_i^{test} \| \quad (13)$$

- MRE (*Mean Relative Error*):

$$MRE = \frac{1}{q} \sum_{i=1}^q \frac{\| \mathbf{y}_i^{test} - \mathbf{d}_i^{test} \|}{\| \mathbf{d}_i^{test} \|} \quad (14)$$

- Max AE (*Max Absolute Error*):

$$Max AE = \max_{i=1 \rightarrow q} \| \mathbf{y}_i^{test} - \mathbf{d}_i^{test} \| \quad (15)$$

For the purpose of estimating 7 parameters of the self-compacting concrete (i.e. the  $SF$ ,  $t_{500}$ ,  $V_{funel}$ ,  $L_{box}$ ,  $J_{ring}$ ,  $SR$  and  $R_{28}$ ), the MLP and TSK networks will have 7 outputs corresponding to the parameters, 5 inputs corresponding to the input parameters of 5 main components (cement, fly ash, water, SD, VMA).

#### 4.1. Results for the MLP network

For an MLP network with known number of inputs and outputs, the remaining main task is to find the number of hidden neurons that allow the network to learn the samples with low value of testing error function as in (5). Using the trial and error method described in previous section, the MLP with 10 hidden neurons was chosen as the one with both learning and testing errors being low.

The results obtained for each parameter using the MLP network are shown above. In Fig. 7 the test results for the  $SF$  (upper) and  $t_{500}$  (lower) parameters are shown for 60 testing cases. We can see that the generated MLP network responses followed the target values for all test cases. The numerical error measures are presented in Tab. 2. In Fig. 8 there were the results for  $V_{funel}$  (top) and  $L_{box}$  (bottom) parameters of the 60 testing cases. We can also see that the generated MLP network responses followed the destination values for all the test cases. The numerical error measures are shown in Tab. 2.

In Fig. 9 there were the results for the parameters  $J_{ring}$  (upper),  $SR$  (middle) and  $R_{28}$  (bottom), each obtained using the MLP network respectively. The selected errors of the approximations are collected in the Tab. 2 below.

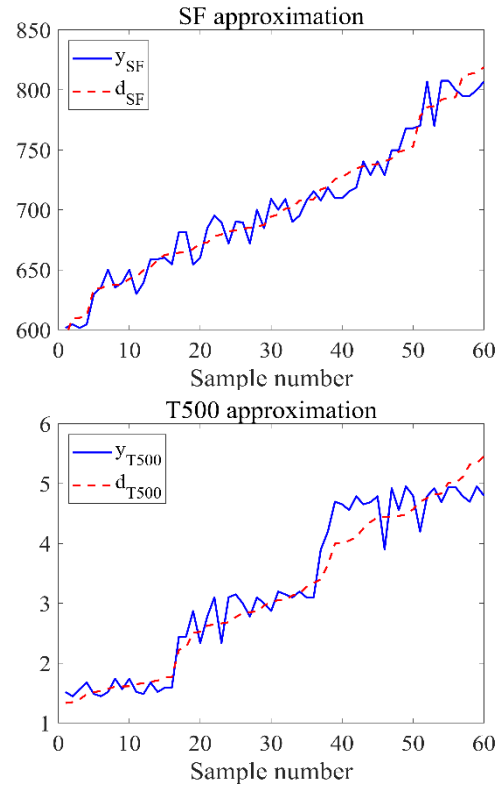


Fig. 7. The approximation results using MLP network for SF and  $t_{500}$  parameters

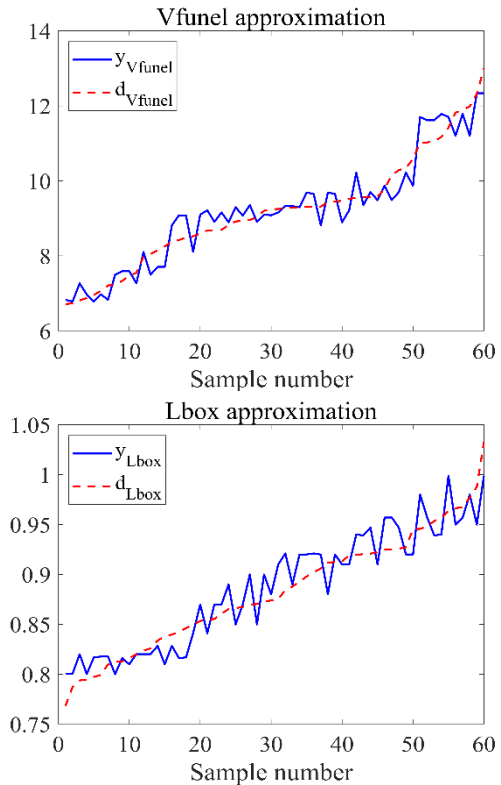


Fig. 8. The approximation results using MLP network for  $V_{funel}$  and  $L_{box}$  parameters

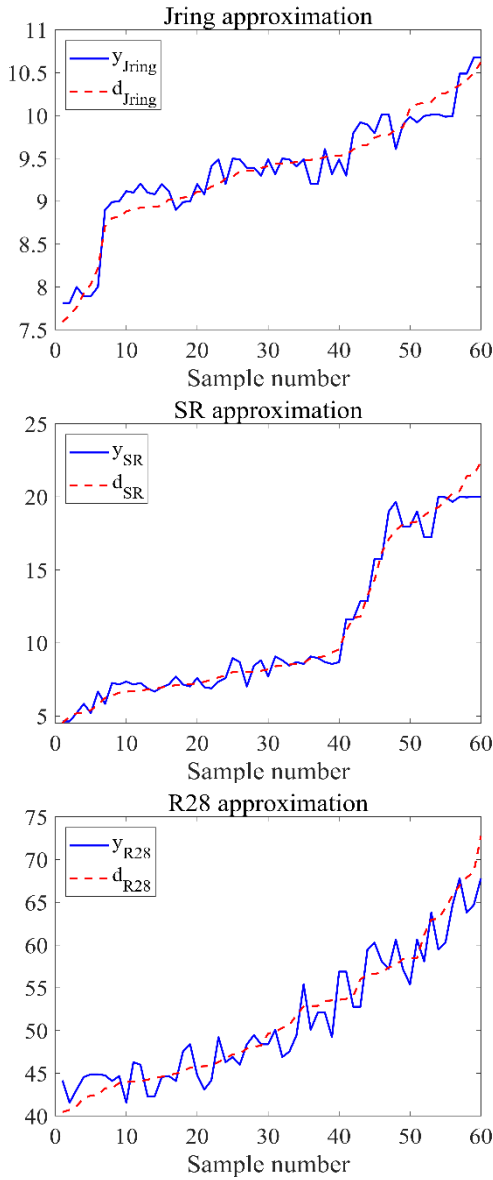


Fig. 9. The approximation results using MLP network for  $J_{ring}$ , SR and  $R_{28}$  parameters

Table 2 Approximation errors of MLP for the parameters

Parameters	MAE	MRE (%)	MaxAE
SF	5.792	0.816	25.392
$t_{500}$	0.0831	2.991	0.535
$V_{funel}$	0.162	1.819	0.485
$L_{box}$	0.0117	1.295	0.0542
$J_{ring}$	0.097	1.022	0.415
SR	0.321	3.572	1.268
$R_{28}$	0.742	1.462	1.875

#### 4.2. Results for the TSK network

In a similar way as the MLP network was trained and selected, for the TSK network with known number of inputs and outputs, the remaining main task is to find the number of reasoning rules that allow the network to learn the samples with low value of testing error function as in (5). With the trial and error method described in previous section, the TSK with 15 rules was selected as the one with both learning and testing errors being low. The achieved results for each parameters using the TSK network are shown below.

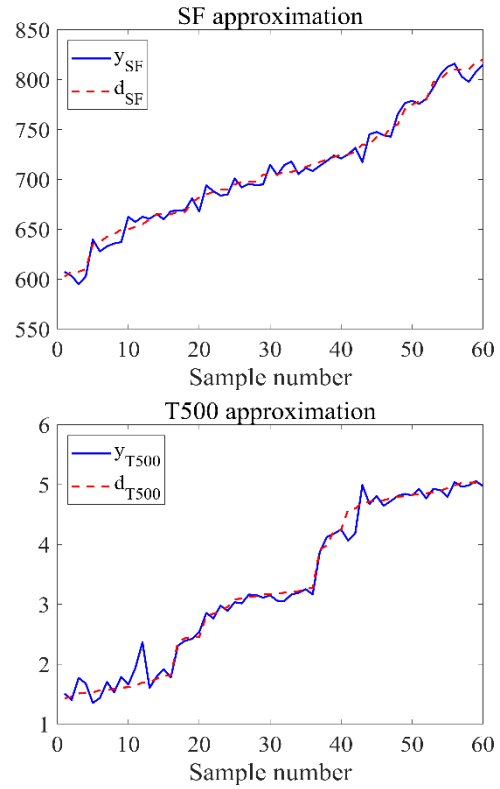


Fig. 10. The approximation results using TSK network for SF and  $t_{500}$  parameters

Figure 10 presented the testing results for the SF (top) and  $t_{500}$  (bottom) parameters. Similar to the results achieved with the application of MLP network, we can see that the generated responses from the TSK network closely followed the destination values for all the 60 test cases. The numerical error measures are presented in Tab. 3.

Figure 11 presented the testing results for  $V_{funel}$  and  $L_{box}$  parameters of the 60 testing cases. Similar to the results achieved with the MLP network shown in Fig. 8, we can see that the generated responses from the TSK network closely followed the destination values for all the 60 test cases. The detailed numerical errors are presented in Tab. 3.

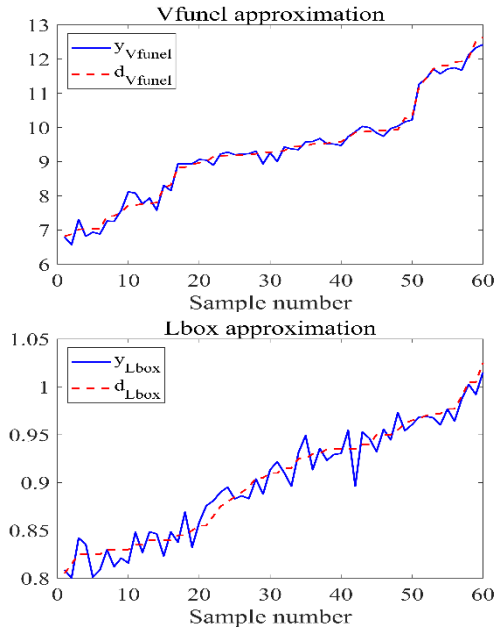


Fig. 11. The approximation results using TSK network for  $V_{funel}$  and  $L_{box}$  parameters

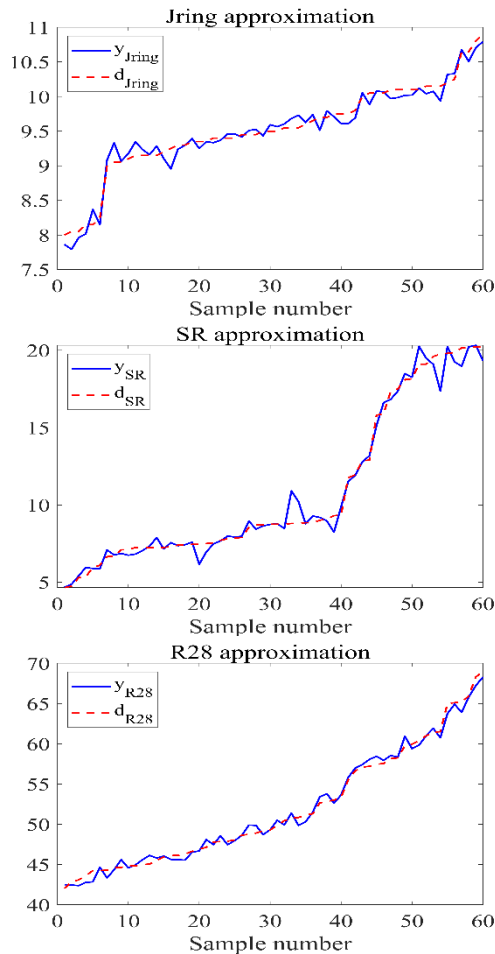


Fig. 12. The approximation results using TSK network for  $J_{ring}$ ,  $SR$  and  $R_{28}$  parameters

Finally, Fig. 12 presented the testing results for  $J_{ring}$  (top),  $SR$  (middle) and  $R_{28}$  (bottom) parameters achieved by using the TSK network respectively. The selected errors of the approximations are collected in the Tab. 3.

Table 3 Approximation errors of TSK for the parameters

Parameters	MAE	MRE (%)	MaxAE
SF	5.198	0.741	29.142
$t_{500}$	0.0744	2.684	0.366
$V_{funel}$	0.0882	0.983	0.273
$L_{box}$	0.0099	1.101	0.0311
$J_{ring}$	0.073	0.779	0.242
$SR$	0.269	2.678	1.417
$R_{28}$	0.466	0.896	2.059

Comparing the results in Tab. 2 and Tab.3 it can be concluded that the TSK achieved a better performance than the MLP but both of the models' results are very satisfactory for us.

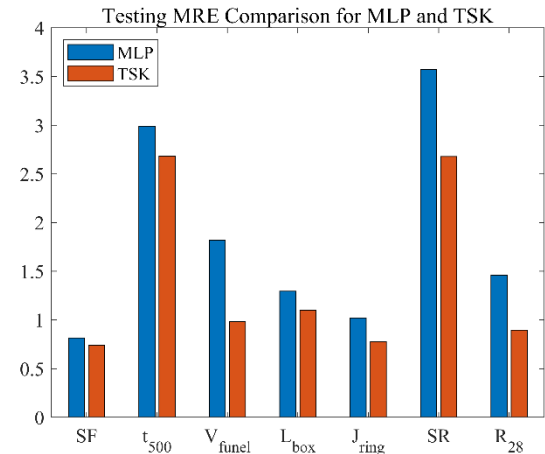


Fig. 13. The comparison of estimation MRE for using MLP and TSK networks

The comparison of the MRE for both proposed networks is shown in Fig. 13, where it can be seen that both networks achieved MRE smaller than 3.6% for all the estimated parameters, however the TSK network's performance was better for each of the parameters.

## 5. CONCLUSIONS

The application of MLP and TSK networks was proposed to estimate the working parameters of the self-compacting concrete based on the input components such as cement, fly ash, water, SD and VMA, and tested with actual real concrete mixtures. Numerical results showed that a high accuracy can

be achieved for all 7 parameters of the SCC by both of the networks, however TSK network showed a better performance than MLP for the data sets used.

The method can be extended for estimation using different concrete components and it can form the base for the inverse problem, where we can find the input mixture components to achieve a given working set of SCC parameters. In practice, these models can help users quickly estimate the expected SCC parameters for a given set of input mixtures, or conversely, determine the input mixtures required to obtain SCC products with certain desired workability parameters.

It should be noted that the proposed models, as for trained models in supervised mode, would need to be re-trained when the data sets expands with new cases that were not similar to the previous ones.

## 6. REFERENCES

- [1] Mindess S., Young J.F., Concrete, Prentice-Hall, Englewood Cliffs, N.J., 1981, pp. 1-671.
- [2] Powers T.C., The Properties of Fresh Concrete, Wiley, N.Y., 1968, pp. 1-664.
- [3] Sobhani J., Najimi M., Pourkhorshidi A.R., Parhizkar T., Prediction of The Compressive Strength Of No-Slump Concrete: A Comparative Study of Regression, Neural Network and ANFIS Models, Construction and Building Materials, Vol. 24, 2010, pp.709-718.
- [4] Yeh I.C., Chen J.W., Modeling Workability of Concrete Using Design Of Experiments And Artificial Neural Networks, J. Technol. , Vol. 20, Issue 2, 2005, pp.153-162.
- [5] TCVN Standard 12209:2018, Self-compacting concrete – Specification and Test Method, 1<sup>st</sup> edition, 2018, pp. 1-22.
- [6] Tattersall G.H., Workability and Quality Control of Concrete, E & FN Spon, London, 1991, pp. 1-272.
- [7] Nguyen T.T., Tran N.L., Vu H.H., Pham T.T., Machine Learning-Based Model for Predicting Concrete Compressive Strength, International Journal of GEOMATE, Vol.20, Issue 77, 2021, pp.197-204.
- [8] Ngandu C., Compressive Strengths Prediction for Concrete with Partial Plastic Fine Aggregate using Neural Network and Reviews, ITECKNE, Vol. 19, No. 1, 2022, pp. 61-68.
- [9] Serraye M., Kenai S., Boukhatem B., Prediction of Compressive Strength of Self-Compacting Concrete (SCC) with Silica Fume Using Neural Networks Models, Civil Engineering Journal, Vol 7, No 1 2021, pp. 118-139.
- [10] Thirumalai R.K., Jayanthi N., Jule Leta Tesfaye, Nagaprasad N., Krishnaraj R., Kaushik V.S., Using an Artificial Neural Network to Validate and Predict the Physical Properties of Self-Compacting Concrete, Hindawi Advances in Materials Science and Engineering, Vol. 2022, pp. 1-10, <https://doi.org/10.1155/2022/1206512>.
- [11] Yousef el Asri, Mouhcine Benaicha, Mounir Zaher, Adil Hafidi Alaoui, Prediction of the compressive strength of self-compacting concrete using artificial neural networks based on rheological parameters, Structural Concrete, 2022, pp. 3696-3717.
- [12] Cheryl R., Bernardo A.L., An Artificial Neural Network Model For The Corrosion Current Density of Steel in Mortar Mixed With Seawater, International Journal of GEOMATE, Vol.16, Issue 56, 2019, pp.79-84.
- [13] Kenneth E., Joenel G.G., Ronaldo S.G., Artificial Neural Network (ANN) Modelling of Concrete Mixed With Waste Ceramic Tiles And Fly Ash, International Journal of GEOMATE, Vol.15, Issue 51, 2018, pp.154-159.
- [14] Widya A., Reni S., Yohannes F., Fadrizal L., Damage Prediction of the Steel Arch Bridge Model Based on Artificial Neural Network Method, International Journal of GEOMATE, Vol.20, Issue 82, 2021, pp.46-52.
- [15] Haykin S., Neural networks and learning machines, 3ed, Prentice Hall, 2009, pp. 1-939.
- [16] Tran H.L., Neural Networks and Their Applications in Signal Processing, HUST Publisher, 2014, pp. 1-213.

---

Copyright © Int. J. of GEOMATE All rights reserved, including making copies unless permission is obtained from the copyright proprietors.

---